New Measurements of the Antineutrino Spin Asymmetry in Beta Decay of the Neutron and Restrictions on the Mass of a Right-handed Gauge Boson

I.A.Kuznetsov, A.P.Serebrov, I.V.Stepanenko, A.V.Alduschenkov, M.S.Lasakov, and A.A.Kokin
Petersburg Nuclear Physics Institute, 188350, Gatchina, Russia
Yu.A.Mostovoi
Kurchatov Institute, 123182, Moscow, Russia
B.G.Yerozolimsky
Department of Physics, Harvard University, Cambridge, Massachusetts, 02138
M.S.Dewey
NIST, Gaithersburg, Maryland 20899

Abstract

We report a new measurement of the neutron antineutrino spin asymmetry coefficient B in the beta decay of polarized neutrons. The work was carried out on the polarized neutron vertical channel of the WWR-M reactor at the Petersburg Nuclear Physics Institute, Gatchina, Russia. Combining results of measurements of the observed asymmetry $P \cdot B = 0.6617 \pm 0.0044$ with measurements of the neutron beam polarization $P = (66.88 \pm 0.22)\%$, we obtain the value $B = 0.9894 \pm 0.0083$. This value implies that the mass of a hypothetical right-handed charged gauge boson in the left-right symmetric model of the weak interaction is greater than 281 GeV/c^2 (90% CL). This is in agreement with restrictions from muon decay and direct searches for an additional vector boson W′.

Precise measurements of neutron beta decay parameters can be used to test the Standard Model of weak interactions. Recently the accuracy of measurements of the neutron lifetime (τ) and electron spin asymmetry (A) have been improved considerably there by improving the accuracy with which the vector and axial vector coupling constants of weak interactions (g_v and g_a) can be derived. However, the vector coupling constant g_v obtained from neutron data is in poor agreement with g_v obtained from superallowed nuclear $0^+ \rightarrow 0^+$ transitions [1,2,3]. Analysis of this discrepancy together with data from ^{19}Ne in the framework of the left-right model of weak interactions is consistent with a finite mass for W_R of 230 GeV/c^2 [2,3]. This is in contradiction with restrictions from muon decay and direct searches for additional vector boson W′[4,5]. A measurement of the antineutrino spin asymmetry in neutron beta decay with an accuracy of less than 1% would be sufficient to strongly confirm or refute this restriction [3].

The work described here was carried out on the vertical channel of cold polarized neutrons at the WWR-M reactor at the Petersburg Nuclear Physics Institute, Gatchina, Russia where the neutron flux is 2×10^8 n/cm^2/sec and the capture neutron flux is 6×10^8 n/cm^2/sec. The maximum wavelength in the spectrum is 4.2 Å.

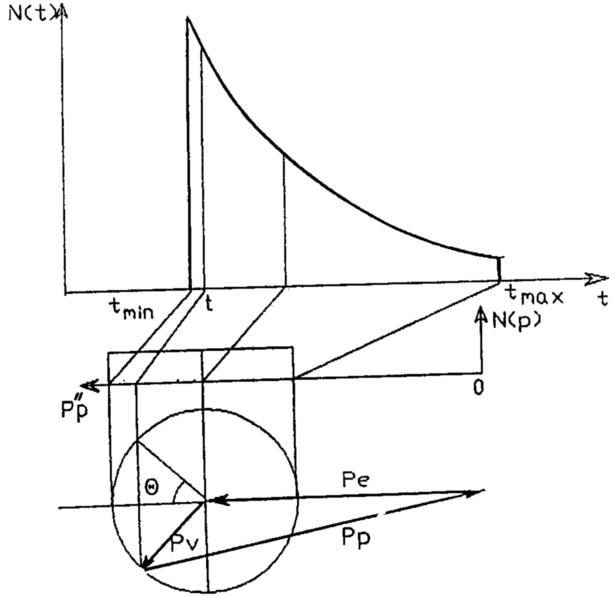

Fig.1. The momentum diagram of neutron decay products and time of flight spectrum of protons for ideal conditions

The scheme for this measurement was first proposed in [6]. Measurements of momentum and angle of escape of the undetected antineutrino are possible due to coincident detection of the electron and recoil proton and subsequent measurement of their momenta. A kinematic diagram of beta decay is shown in Fig.1. From the known neutron decay energy and the measured electron energy, the antineutrino energy can be deduced with an accuracy of better than 0.75 keV, the maximum proton recoil energy. For a given electron momentum, all possible values of antineutrino momentum lie on a sphere of radius $p_{\bar{\nu}} = (E_0 - E_e)/c$, where $p_{\bar{\nu}}$ is antineutrino momentum, E_0 is the total kinematic energy of decay, and E_e is the electron energy. By further measuring the parallel projection of proton momentum $p_{\|}$ using time of flight, we can determine the antineutrino escape angle and reconstruct the beta decay event.

The events detected in this experiment can be assigned to a matrix of coincidence with coordinates E_e and t_p for the two opposite directions of beam polarization (+ and −). The event rate for each cell of this matrix is given by:

$$N_{ik}^{\pm} = f(E_i)\left[1 + a \cdot \frac{v_i}{c} \cdot <\cos\Theta_{e\bar{\nu}}>_{ik} \pm P \cdot A \cdot \frac{v_i}{c} \cdot <\cos\Theta_{\sigma e}>_{ik} \pm \right.$$
$$\left. \pm\, P \cdot B \cdot <\cos\Theta_{\sigma\bar{\nu}}>_{ik}\right] \qquad (1)$$

taking into account the correlation coefficients of beta decay. This yields the experimental asymmetry:

$$X_{ik} \equiv \frac{N_{ik}^{+} - N_{ik}^{-}}{N_{ik}^{+} + N_{ik}^{-}} = \frac{P \cdot A \cdot \frac{v_i}{c} \cdot <\cos\Theta_{\sigma e}>_{ik} + P \cdot B \cdot <\cos\Theta_{e\bar{\nu}}>_{ik}}{1 + a \cdot \frac{v_i}{c} \cdot <\cos\Theta_{e\bar{\nu}}>_{ik}}, \qquad (2)$$

and finally:

$$(P \cdot B)_{ik} = \frac{\left[X_{ik}(1 + a \cdot \frac{v_i}{c} \cdot <\cos\Theta_{e\bar{\nu}}>_{ik})\right] - A \cdot P \cdot \frac{v_i}{c} \cdot <\cos\Theta_{\sigma e}>_{ik}}{<\cos\Theta_{\sigma\bar{\nu}}>_{ik}}. \qquad (3)$$

In these equations a, A, and B are coefficients of electron antineutrino asymmetry, electron spin asymmetry, and antineutrino spin asymmetry, P is the degree of neutron polarization, v is the electron velocity, and $f(E_i)$ combines the phase-space factor and Fermi function. The subscripts i and k denote a definite interval of electron energy E_i and time of flight of the proton t_k. To determine B it is necessary to know the beam polarization and calculated values for $\frac{v}{c}$ $<\cos\Theta_{e\bar{\nu}}>$, $\frac{v}{c}$ $<\cos\Theta_{\sigma e}>$ and $<\cos\Theta_{\sigma\bar{\nu}}>$. The values of the correlation coefficients a and A are known from previous experiments [7,8]. The terms with coefficients a and A are small (0.1), so the experimental uncertainties on a and A do not contribute significantly to the total error of $P \cdot B$.

To calculate the mean cosine values, a Monte Carlo model of the beta decay process inside the apparatus is used. The model includes all the necessary geometrical parameters of the chamber, the responses of the electron and proton detectors, the distribution of neutron intensity inside the beam (this was measured in a separate experiment), the shape of the electron spectrum in the form of the Fermi function, and the characteristics of the amplitude to digital (ADC) and time to digital (TDC) converters. A relaxation calculation is used to obtain the electric field inside the apparatus.

A diagram of the apparatus is shown in Fig.2.

The decay region (4) is defined by means of a special diaphragm in front of the electron detector. Coincident signals from the electron (1) and proton (2) detectors, which are located on opposite sides of the decay region, are registered for each direction of neutron polarization.

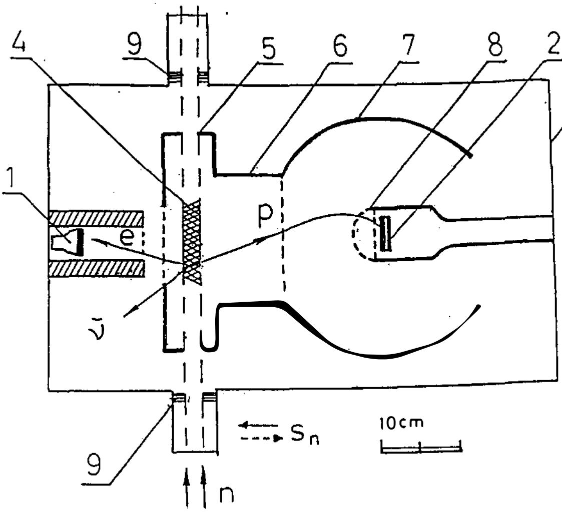

Fig.2. Experimental apparatus. 1- electron detector; 2- proton detector; 3- vacuum chamber; 4- decay region; 5- cylindrical electrode; 6- TOF electrode; 7- spherical electrode; 8- spherical grid; 9- LiF diaphragm

The electron detector is a photomultiplier with a plastic scintillator (diam 75 mm and thickness 3 mm). The energy resolution and fraction of backscattering of electrons for this detector were determined in a separate experiment by means of a magnetic beta spectrometer [8].

Decay protons passing through the time of flight cylinder (6) at first maintain their velocities. Then they are accelerated and focused onto the proton detector by an electric field with potential 25.6 kV applied between the spherical electrode (7) and spherical grid (8). The proton detector is an assembly of two microchannel plates. The diameter of the detector is 65 mm. In this configuration, it is possible to determine the time of arrival of each proton to an accuracy of 10 nsec.

The entire chamber is surrounded by three pairs of current carrying frames to null the earth's magnetic field and to provide a 0.05 mT guiding magnetic field in the chamber. The residual earth's field is less than 1 μT. The polarization reversal is accomplished with a radio frequency flipper. To avoid any possible influence of the flipper on the photomultiplier, the guiding magnetic field and the magnetic field of the flipper are reversed from time to time.

Pulses from the electron detector are used to start a TDC and to provide the electron energy. Pulses from the proton detector stop the TDC thereby providing a time of flight measurement. The method of delayed coincidence is used to determine the background. The background is measured simultaneously with the coincidence signal using the same electronic processing. During 93 hours of acquisition time, a total of 393057 decay events were registered. The signal to noise ratio in the area under the time of flight spectrum was 1.5 to 1.

The electron energy detector is calibrated at the beginning and end of every run. This is done to correct for possible gain shifts of the photomultiplier. Calibrations are carried out with the help of two calibrated electron sources ^{113}Sn (357 keV) and ^{137}Cs (617 keV).

Comparisons of experimental results and calculations for both time and energy spectra are shown in Fig.3.

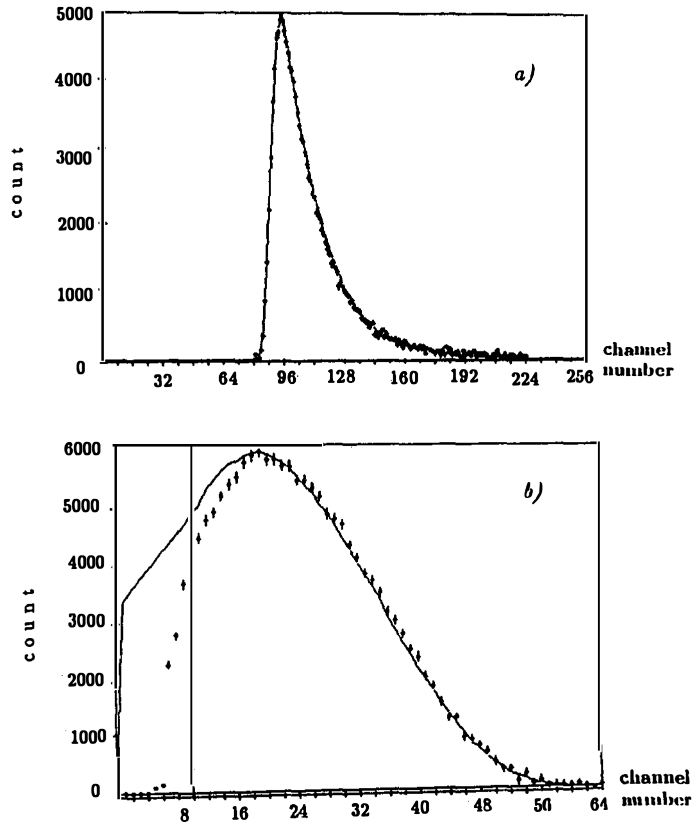

Fig.3. Comparison of experimental and simulated spectra;
(a) time of flight spectra; (b) energy spectra.
Circles are experimental points, solid curve is computer simulation

The proton time of flight spectrum is integrated over energy and polarization states while the energy spectrum is integrated over time and polarization states. There is good agreement between experimental and calculated time of flight spectra ($\chi^2/(N-1) = 1.15$). However, the agreement between the energy spectra in the region of low energy is poor, possibly due to nonlinearities in the electronics in this region. Analysis of the experimental data shows that this discrepancy does not influence the final result.

We follow several steps to extract $P \cdot B$ from the data. First we match, in software, the offsets and gains, both for time and energy, between the Monte Carlo and experimentally observed matrices $N^+_{ik} + N^-_{ik}$. Next we rebin both the theoretical and experimental spectra by energy interval (i) and *fixed fraction* of the timing curve ($\tilde{k}$). In this scheme $\tilde{k} = 1$ might correspond to the fastest 5% of events recorded, $\tilde{k} = 2$ the next fastest 7%, etc. This is done because $< \cos\Theta_{\sigma\bar{\nu}} >_{i\tilde{k}}$ is essentially independent of i. Averaging over energy (i), we obtain $P \cdot B$ as a function of $\cos\Theta_{\sigma\bar{\nu}}$ (see Fig.4).

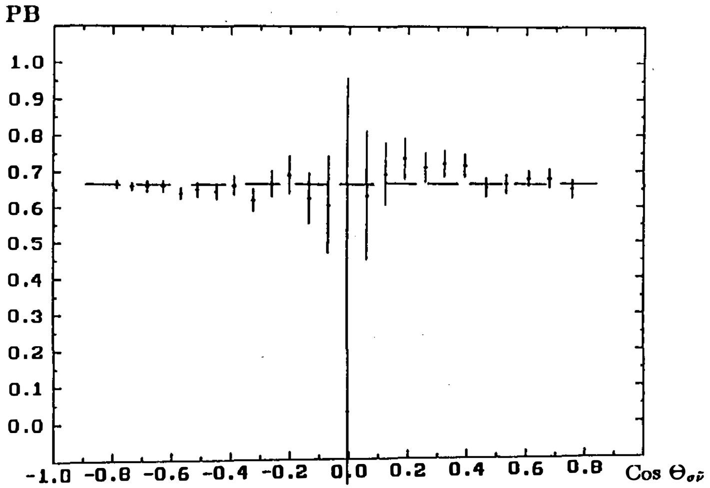

Fig.4. Dependence of B on $\cos\Theta_{\sigma\bar{\nu}}$

The average value $P \cdot B = 0.6617 \pm 0.0044$ and $\chi^2/(N-1) = 0.78$.

Statistically combining these results, we obtain $P \cdot B = 0.6617 \pm 0.0044$ for $\chi^2/(N-1) = 0.78$.

Possible systematic errors in this experiment are analyzed by varying model parameters in the Monte Carlo by an amount equal to the experimental uncertainty on those parameters. The varied parameters include the resolution of electron detector, the size of the energy channel, the placement of zero in the energy scale, the intensity of the backscattering tail, geometrical sizes, and uncertainties in the correlation coefficients a and A (see Table).

Table. Final 1-sigma absolute uncertainties on B. The total systematic error is the quadrature sum of the individual errors. The total absolute error is the quadrature sum of the systematic, polarization, and statistical errors.

Source of Uncertainty	Nominal value	ΔB
^{113}Sn position (channels)	18.25±0.3	0.0026
Energy resolution of electron detector (keV)	34.5±1.7	0.0020
Size of energy channel (keV)	10.75±0.13	0.0007
Electron backscattering fraction	0.06±0.02	0.0012
Radius of proton detector diaphragm (mm)	130.0±0.25	0.0004
Radius of electron detector (mm)	37.5±0.25	0.0001
Radius of electron detector diaphragm (mm)	45.0±0.25	0.0006
Electron neutrino asymmetry coefficient (a)	0.1017±0.0051	0.0010
Total systematic error		0.0038
Polarization error		0.0033
Statistical error		0.0066
Total absolute error		0.0083

From the analysis we conclude that the total systematic error on our result is 0.0038. The largest source of uncertainty (±0.0021) is due to the low energy resolution of electron detector (25% for 115 keV).

The polarization of the neutron beam was measured using a new high precision technique. This method and its result are described in detail in [9]. In these measurements both the beam velocity spectrum and angular distribution are taken into account. The measured wavelength-dependent polarization is averaged with the time of flight spectrum through the apparatus. An additional correction is made to take into account the spectral dependence of the neutron spin flipper efficiency. The polarization measurements were carried out simultaneously with the measurement of B. From these measurements a value of polarization was obtained: $P = 0.6688 \pm 0.0022$. Using the value of $P \cdot B$ and P, we find: $B = 0.9894 \pm 0.0083$. The accuracy of this result is 4.5 times better than the previous measurement [8].

The antineutrino spin asymmetry B is not sensitive to influences from the strong interactions, from renormalization of the axial vector constant, and from influences of radiative corrections. B varies from 0.988 by less than 0.001 when it is evaluated according to $V - A$ theory using the discrepant values of λ from different experiments. As a consequence of this, it is possible to place a restriction on the mass of W_R using B alone. In the left-right symmetric model with zero mixing angle one has $B = (1 - 2\delta^2)B_{V-A}$ where δ is the squared ratio of left- to right-handed boson masses. For this deviation, our measured value with its accuracy of 0.84% constrains M_{W_R} to be greater than or equal to 281 GeV/c^2 (90% CL). General restrictions in the squared mass ratio (δ) mixing angle (ζ) plane arising from this experimental result are shown in Fig.5. The figure includes experimental results for the neutron lifetime, neutron electron spin asymmetry, lifetime for $0^+ \rightarrow 0^+$ transitions, and lifetime and asymmetry in ^{19}Ne, which together suggest a mass of about 230 GeV/c^2 for W_R. The results of this direct neutron beta decay experiment fail to confirm the existence of a finite δ at zero mixing angle.

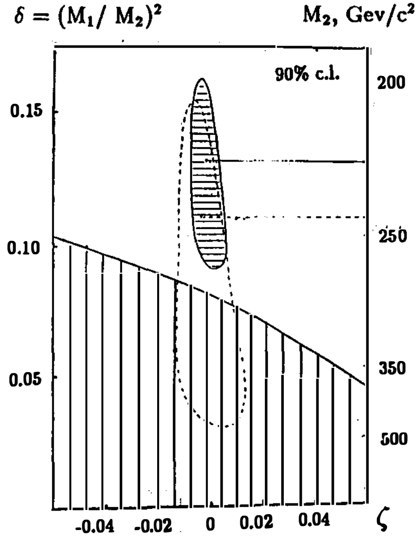

Fig.5. Restrictions on the left-right symmetric model from different experimental data. (1) The horizontally shaded region comes from measurements of λ_τ and λ_A in the neutron and ^{19}Ne systems; (2) the region surrounded by a dotted line is the same except that data from Ref.[8] is not used; (3) the vertically shaded region comes from the present measurement

The accuracy of this result can be improved with more statistics since the systematic errors in this experiment are smaller than the statistical errors. One might hope to improve the statistical accuracy of this experiment to 0.2%, which is comparable with the accuracy of the polarization determination. As discussed in Ref.[9], the accuracy of polarization can be improved to 0.1% if supermirrors are used to prepare the beam polarization. The systematic error can be decreased using of new silicon detector to improve the energy resolution. With these improvements, it should be possible to improve this mass limit to 500 GeV/c^2.

This work was supported by ISF Grant No. 59000 and Grant No. 93-02-14382 of the Russian Fund of Fundamental Research.

References

[1] D. Dubbers, W. Mampe, and J. Döhner, Europhys. Lett. **11**, 195 (1990).

[2] A. S. Carnoy, J. Deutsch, T. A. Girard, and R. Prieels, Phys. Rev. Lett. **65**, 3249 (1990).

[3] A. P. Serebrov and N. V. Romanenko, JETP Lett. **55**, 503 (1992).

[4] A. Jodidio et al., Phys. Rev. D **34**, 1967 (1986).

[5] UA2 Collaboration, Nucl. Phys. B **400**, 3 (1993).

[6] B. G. Erozolimsky, Y. A. Mostovoi, and A. I. Frank, Preprint IAE-3180, 1979, I. V. Kurchatov Institute of Atomic Energy, Moscow.

[7] C. Stratowa, R. Dobrozemsky, and P. Weinzierl, Phys. Rev. D **18**, 3970 (1978).

[8] B. G. Erozolimskii, I. A. Kuznetsov, I. A. Kuida, Y. A. Mostovoi, and I. V. Stepanenko, Sov. J. Nucl. Phys. **52**, 999 (1990).

[9] A. P. Serebrov, A. V. Aldushchenkov, M. S. Lasakov, I. A. Kuznetsov, and I. V. Stepanenko, New method for precise determination of neutron beam polarization, (to be published).